From Planck data to Planck era:
Observational tests of Holographic Cosmology

Niayesh Afshordi,[1,2] Claudio Corianò,[3,4,5] Luigi Delle Rose,[3,6,7] Elizabeth Gould,[1,2] and Kostas Skenderis[3,4]

[1]*Perimeter Institute for Theoretical Physics, 31 Caroline St. N., Waterloo, ON, N2L 2Y5, Canada*
[2]*Department of Physics and Astronomy, University of Waterloo, Waterloo, ON, N2L 3G1, Canada*
[3]*STAG Research Centre, Highfield, University of Southampton, SO17 1BJ Southampton, UK*
[4]*Mathematical Sciences, Highfield, University of Southampton, SO17 1BJ Southampton, UK*
[5]*Dipartimento di Matematica e Fisica "Ennio De Giorgi",*
Università del Salento and INFN-Lecce, Via Arnesano, 73100 Lecce, Italy
[6]*School of Physics and Astronomy, Highfield, University of Southampton, SO17 1BJ Southampton, UK*
[7]*Rutherford Appleton Laboratory, Chilton, Didcot, OX11 0QX, UK*
(Dated: January 4, 2017)

We test a class of holographic models for the very early universe against cosmological observations and find that they are competitive to the standard ΛCDM model of cosmology. These models are based on three dimensional perturbative super-renormalizable Quantum Field Theory (QFT), and while they predict a different power spectrum from the standard power-law used in ΛCDM, they still provide an excellent fit to data (within their regime of validity). By comparing the Bayesian evidence for the models, we find that ΛCDM does a better job globally, while the holographic models provide a (marginally) better fit to data without very low multipoles (i.e. $l \lesssim 30$), where the dual QFT becomes non-perturbative. Observations can be used to exclude some QFT models, while we also find models satisfying all phenomenological constraints: the data rules out the dual theory being Yang-Mills theory coupled to fermions only, but allows for Yang-Mills theory coupled to non-minimal scalars with quartic interactions. Lattice simulations of 3d QFT's can provide non-perturbative predictions for large-angle statistics of the cosmic microwave background, and potentially explain its apparent anomalies.

Observations of the cosmic microwave background (CMB) offer a unique window into the very early Universe and Planck scale physics. The standard model of cosmology, the so-called ΛCDM model, provides an excellent fit to observational data with just six parameter. Four of these parameters describe the composition and evolution of the Universe, while the other two are linked with the physics of the very early Universe. These two parameters, the tilt n_s and and the amplitude $\Delta_0^2(q_*)$, parameterize the power spectrum of primordial curvature perturbations,

$$\Delta_{\mathcal{R}}^2(q) = \Delta_0^2(q_*) \left(\frac{q}{q_*}\right)^{n_s-1}, \qquad (1)$$

where q_*, the pivot, is an an arbitrary reference scale. This form of the power spectrum is a good approximation for slow-roll inflationary models and has the ability to fit the CMB data well. Indeed, a near-power-law scalar power spectrum may be considered as a success of the theory of cosmic inflation.

The theory of inflation is an effective theory. It is based on gravity coupled to (appropriate) matter perturbatively quantized around an accelarating FLRW background. At sufficiently early times the curvature of the FLRW spacetime becomes large and the perturbative treatment is expected to break down – in this regime we would need a full-fledged theory of quantum gravity. One of the deepest insights about quantum gravity that emerged in recent times is that it is expected to be holographic [1–3], meaning that there should be an equivalent description of the bulk physics using a quantum field theory with no gravity in one dimension less. One may thus seek to use holography to model the very early Universe.

Holographic dualities were originally developed for spacetimes with negative cosmological constant (the AdS/CFT duality) [3] and soon afterwards the extension to de Sitter and cosmology was considered [4–8]. In this context, the statement of the duality is that the partition function of the dual QFT computes the wavefunction of the universe [8] and using this wavefunction cosmological observables may be obtained. Alternatively, [9–13], one may use the Domain-wall/Cosmology correspondence [14]. The two approaches are equivalent [15].

Holography offers a new framework that can accommodate conventional inflation but also leads to qualitatively new models for the very early universe. While conventional inflation corresponds to a strongly coupled QFT [16–32], the new models are associated with a weakly coupled QFT. These models correspond to a non-geometric bulk, and yet holography allows us to compute the predictions for the cosmological observables. We emphasise that the application of holography to cosmology is conjectural, the theoretical validity of such dualities is still open and different authors approach the topic in different ways. Here we seek to test these ideas against observations.

A class of non-geometric models were introduced in [9] and their prediction have been worked out in [9–13, 33, 34]. These models are based on three dimensional super-renormalizable QFT and they universally predict a scalar

power spectrum of the form,

$$\Delta_{\mathcal{R}}^2(q) = \frac{\Delta_0^2}{1 + (gq_*/q)\ln|q/\beta gq_*| + \mathcal{O}(gq_*/q)^2}, \quad (2)$$

where g is related to the coupling constant of the dual QFT, while β depends on the parameters of the dual QFT (see below).

The form of the power spectrum in (2) is distinctly different from (1)[1]. Since these are qualitatively different parametrizations, one may ask which of the two is preferred by the data. Note that this question is *a priori* independent of the underlying physical models that produced (1) and (2). This question has already been addressed for WMAP7 data [37] in [35, 38] and it was found that while the data mildly favour ΛCDM, it was insufficient to definitively discriminate between the two cases. Since then, the Planck mission has released its data [39] and it is now time to revisit this issue. We will present the main conclusions of the fit to Planck data here, referring to [40] for a more detailed discussion.

On the theoretical side, there has also been significant progress since [35]. While the form of (2) is universally fixed, the precise relation between g and β and the parameters of the dual QFT requires a 2-loop computation, which has now been carried out in [41]. We can thus not only check whether (2) is compatible with CMB data, but also use the data to do a model selection.

Theory.— Following [9], we consider the dual QFT to be $SU(N)$ gauge theory coupled to scalars Φ^M and fermions ψ^L, where M, L are flavor indices. The action is given by

$$S = \frac{1}{g_{\mathrm{YM}}^2}\int d^3x\, \mathrm{tr}\left[\frac{1}{2}F_{ij}F^{ij} + (\mathcal{D}\Phi)^2 + 2\bar{\psi}\slashed{\mathcal{D}}\psi \right.$$
$$\left. + 2\sqrt{2}\mu\cdot(\Phi\bar{\psi}\psi) + \frac{1}{6}\lambda\cdot\Phi^4\right], \quad (3)$$

where all fields, $\varphi = \varphi^a T^a$, are in the adjoint of $SU(N)$ and $\mathrm{tr}T^a T^b = \frac{1}{2}\delta^{ab}$. F_{ij} is the Yang-Mills field strength, and $\mathcal{D}$ is a gauge covariant derivative. We use the shorthand notation $(\mathcal{D}\Phi)^2 = \delta_{M_1 M_2}\mathcal{D}_i\Phi^{M_1}\mathcal{D}^i\Phi^{M_2}$, $\bar{\psi}\slashed{\mathcal{D}}\psi = \delta_{L_1 L_2}\bar{\psi}^{L_1}\gamma^i\mathcal{D}_i\psi^{L_2}$, $\mu\cdot(\Phi\bar{\psi}\psi) \equiv \mu_{ML_1L_2}\Phi^M\bar{\psi}^{L_1}\psi^{L_2}$ and $\lambda\cdot\Phi^4 \equiv \lambda_{M_1 M_2 M_3 M_4}\Phi^{M_1}\Phi^{M_2}\Phi^{M_3}\Phi^{M_4}$.

The holographic dictionary relates the scalar and tensor power spectra to the 2-point function of the energy-momentum tensor T_{ij}. For the scalar power spectrum,

$$\Delta_{\mathcal{R}}^2(q) = \frac{1}{4\pi^2 N^2 f(g_{\mathrm{eff}}^2)}, \quad (4)$$

where $g_{\mathrm{eff}}^2(q) \equiv g_{\mathrm{YM}}^2 N/q$ is the effective dimensionless 't Hooft coupling constant, q is the magnitude of the momentum $\vec{q}$ and $f(g_{\mathrm{eff}}^2)$ is extracted from the momentum space 2-point of function of the trace of the energy momentum tensor, $\langle T_i^i(\vec{p})T_j^j(\vec{q})\rangle = (2\pi)^3\delta(\vec{p}+\vec{q})q^3 N^2 f(g_{\mathrm{eff}}^2)$. In perturbation theory,

$$f(g_{\mathrm{eff}}^2) = f_0\left[1 - f_1 g_{\mathrm{eff}}^2 \ln g_{\mathrm{eff}}^2 + f_2 g_{\mathrm{eff}}^2 + \mathcal{O}(g_{\mathrm{eff}}^4)\right]. \quad (5)$$

The function f_0 is determined by a 1-loop computation, while f_1 and f_2 come from 2-loops. The presence of the logarithm is due to UV and IR divergences in the computation of the 2-point function of the energy momentum tensor. A detailed derivation of (4) may be found in [10, 35]. Following [35], (2) and (4-5) match if:

$$gq_* = f_1 g_{\mathrm{YM}}^2 N, \ln\frac{1}{\beta} = \frac{f_2}{f_1} + \ln|f_1|, \Delta_0^2 = \frac{1}{4\pi^2 N^2 f_0}. \quad (6)$$

So, a universal prediction of these class of theories is the power spectrum (2), independent of the details of the 2-loop computation[2].

The 1-loop computation was done in [9, 10] and we here report the result of the 2-loop computation [41] – a summary of the computation is provided in the appendix.. The final result is

$$f_0 = \frac{1}{64}\mathcal{N}_{(B)}, \quad \mathcal{N}_{(B)} = 1 + \sum_M (1 - 8\xi_M)^2 \quad (7)$$

$$f_1 = -\frac{4}{3\pi^2}\frac{1}{\mathcal{N}_{(B)}}\left(\mathcal{N}_\psi - 2 + 2\mathcal{N}_\Phi + \frac{1}{2}\mu^2 - 48\,\Sigma_\Phi\right) (8)$$

$$\ln\beta = \ln\frac{1}{|g|} - \frac{a_0}{f_1} - \frac{64/\pi^2}{f_1\mathcal{N}_{(B)}}\Sigma_\Phi\ln\frac{Nf_1}{g} \quad (9)$$

where $\mathcal{N}_\Phi$ and $\mathcal{N}_\psi$ are the total number of scalars and fermions, and

$$a_0 = -\frac{1}{24\pi^2\mathcal{N}_{(B)}}\Big[16 + 3\pi^2 - 56\mathcal{N}_\psi - 4\sum_M \mu_{MM}^2 +$$

$$\sum_M 3(8\xi_M - 1)(8\left(\pi^2 - 16\right)\xi_M - 3\pi^2 + 112 + 2\mu_{MM}^2)$$

$$+\pi^2\sum_{M_1,M_2}\lambda_{M_1 M_1 M_2 M_2}(8\xi_{M_1} - 1)(8\xi_{M_2} - 1)\Big],$$

$$\Sigma_\Phi = \sum_M \xi_M^2\left(2 + \frac{1}{2}\mu_{MM}^2\right),$$

where $\mu_{M_1 M_2}^2 = \sum_{L_1,L_2}\mu_{M_1 L_1 L_2}\mu_{M_2 L_2 L_1}$, ξ_M is the non-minimality parameter[3] and summations over $M(L)$ are over scalars (fermions).

---

[1] For small enough g, one may rewrite (2) in the form (1) with momentum dependent $n_s(q)$. However, as discussed [9, 35], the momentum dependence of $n_s(q)$ is qualitatively different from that of slow-roll inflationary models [36].

---

[2] This assumes $f_1 \neq 0$. A separate analysis is required, where $f_1 = 0$, e.g., for (3) without gauge fields and fermions.

[3] Non-minimal scalars on a curved background have the coupling $1/(2g_{\mathrm{YM}}^2)\sum_M\int\xi_M R(\Phi^M)^2$, where R is the curvature scalar, and this term induces an "improvement term" to their energy momentum tensor, $T_{ij} = (2/\sqrt{g})(\delta S/\delta g^{ij})|_{g_{ij}=\delta_{ij}}$, see [42].

Fitting to data.— We would like now to assess how well a power spectrum of the form (2) fits the cosmological data and compare with that of the conventional power-law power spectrum. Recall that ΛCDM is parametrized by six parameters, $(\Omega_b h^2, \Omega_c h^2, \theta, \tau, \Delta_0^2, n_s)$, where $\Omega_b h^2$ and $\Omega_c h^2$ are the baryon and dark matter densities, θ is the angular size of the sound horizon at recombination, τ is the the optical depth due to re-ionization and Δ_0^2, n_s are the parameters entering in (1). To formalize the comparison, we define (following [35]) holographic cosmology (HC) as the model parametrized by $(\Omega_b h^2, \Omega_c h^2, \theta, \tau, \Delta_0^2, g, \ln \beta)$.[4] This model has 7 parameters so in order to compare models with the same number of parameters we also consider ΛCDM with running $\alpha_s = dn_s/d\ln q$. Note that our aim here is to compare *empirical models*, not the underlying physical models that lead to them. If the data selects one of the two empirical models, then this would falsify all physical models that underlie the other model.
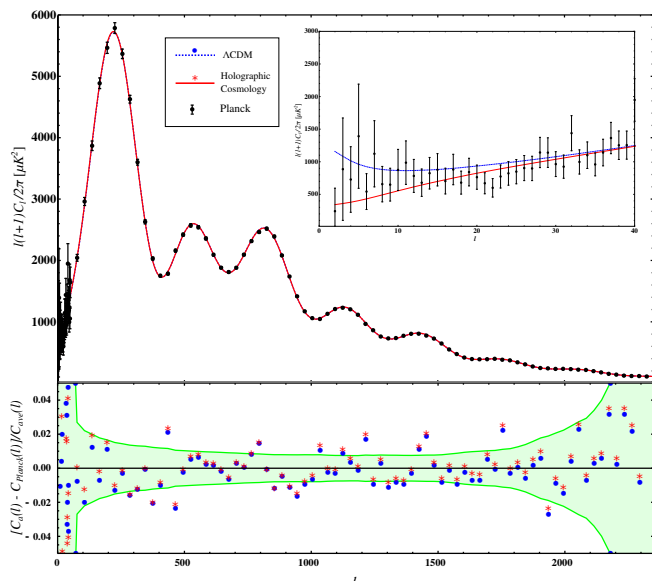

FIG. 1. Angular power spectrum of CMB temperature anisotropies, comparing Planck 2015 data with best fit ΛCDM (dotted/blue) and holographic cosmology (solid/red) models, for $l \geq 30$. Lower panel shows the relative residuals, where the green shaded region indicates the 68% region of Planck 2015 data.

We analysed the data using CosmoMC [43–49]. We ran both ΛCDM and HC with the same datasets, fitting the models to the Planck 2015 data including lensing [39, 50–55], as well as Baryonic Acoustic Oscillations

---

[4] In [35] the parameter β was incorrectly assumed to be equal one. We refitted the WMAP data and found that the global minimum is at $\beta = 3.777$.

TABLE I. Upper part: Planck 2015+BAO+BKP mean parameters for holographic cosmology. Lower part: χ^2 values for fit with all multipoles and fit with $l < 30$ multipoles excluded.

HC	$10^9 \Delta_0^2$	g	$\ln \beta$
all l	$2.126^{+0.058}_{-0.058}$	$-0.00703^{+0.00105}_{-0.00167}$	$0.877^{+0.186}_{-0.239}$
$l \geq 30$	$2.044^{+0.072}_{-0.075}$	$-0.01305^{+0.00452}_{-0.00345}$	$1.014^{+0.206}_{-0.272}$

	HC	ΛCDM	ΛCDM running
χ^2 (all l)	11324.5	11319.9	11319.6
$\chi^2 (l \geq 30)$	824.0	824.5	823.5

(BAO) [56–63] and BICEP2-Keck-Planck (BKP) polarization [64]. After CosmoMC had run to determine the mean and errors in the parameters, we ran the minimizer [65] within the code to determine the best fit parameters and likelihood.

The Planck angular TT spectrum together with the best fit curves and residuals for HC and ΛCDM are presented in Fig. 1. Notice that the difference between ΛCDM and HC lies within the 68% region of Planck, with the largest difference being at small multipoles. Very similar results hold for the TE and EE spectra [40]. We determined the best fit values for all parameters for HC, ΛCDM and ΛCDM with running. Our values for the parameters of ΛCDM and ΛCDM with running are in agreement with those determined by the Planck team. All common parameters of the three models are within 1σ of each other (with the notable exception of the optical depth τ [40]). We report the values of $\Delta_0, g, \ln \beta$ and χ^2 in Table I (the list of all parameters can be found in [40]). The χ^2 of the fit indicates that HC is disfavoured at about 2.2σ relative to ΛCDM with running, when we consider all multipoles.

Relative to the WMAP fit in [35] the value of g has decreased from -1.3×10^{-3} to -7×10^{-3}. In Fig. 2, we investigate how the value of g changes if we change the range of multipoles that we consider. It is clear from the plot that the value of g is compatible between WMAP and Planck, if we keep the same multipoles. It is also clear that the high l modes want to push g to lower negative values. Larger values of $|g|$ indicate that the theory may become non-perturbative at very low l and, as such, the predictions of the model cannot be trusted in that regime. We shall see below that this is supported by model selection criteria. Therefore, we repeat the fitting, excluding the $l < 30$ multipoles. The results for $\Delta_0, g, \ln \beta$ and χ^2 are tabulated in Table I. With this data, all common parameters are now compatible with each other [40]. The χ^2 test shows that the three models are now within 1σ.

The power spectrum for the tensors takes the same form as (2) but with different values of g and β. We fitted the data with this form of the power spectrum and found that it is consistent with $r = 0$; the 2σ upper limit on the tensor-to-scalar ratio is $r < 0.125$.
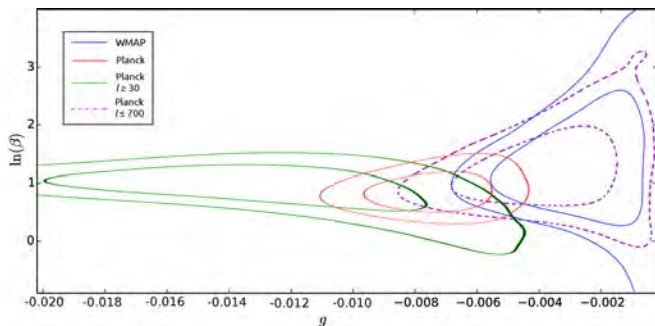
FIG. 2. Plot of 1σ and 2σ regions in parameter space for holographic cosmology g and $\ln(\beta)$ values for WMAP (blue, right), Planck (red, middle), Planck with $l < 30$ values removed (green, left), and Planck with $l > 700$ values ignored (purple, dashed). We see that higher resolution data progressively pushes g to lower negative values.

Bayesian Evidence.— In comparing different models, one often uses information criteria such as the value of χ^2, which quantifies the goodness of a fit. We emphasise that with "model" we mean the three empirical models introduced above, ΛCDM, ΛCDM with running and HC. What we really want to know, however, is what is the probability for each of these models given the data. This is obtained by computing the Bayesian Evidence.

As discussed in [35], if we assume flat priors for all parameters α_M that define a given model, the Bayesian evidence is given by $E = \frac{1}{\mathrm{Vol}_M} \int d\alpha_M \mathcal{L}(\alpha_{\mathcal{M}})$, where $\mathcal{L}(\alpha_{\mathcal{M}})$ is the likelihood and Vol_M is the volume of the region in parameter space over which the prior probability distribution is non-zero. The evidence may be computed either by using CosmoMC or by MultiNest [66–68].

Note that the aim here is to compare empirical models and we determined the priors from previous fits of the same empirical models to data (as is common)[5]. We use the priors in Table 4 of [35], except that the upper limit of $100\,\theta$ is taken to be 1.05. The prior for the running is taken to be $|\alpha_s| \leq 0.05$. The priors for n_s are the asymmetric prior used in [35]: $0.92 \leq n_s \leq 1$. For the prior for g we use variable range, $g_{\min} \leq g < 0$. This prior is fixed by the requirement that perturbation theory is valid. We will allow for the possibility that the perturbative expansion is valid only for $l > 30$. We use as a rough estimate for the validity of perturbation theory that gq^*/q is sufficiently small, taking this to mean a value between 0.20 and 1 at $l = 30$[6]. This translates into

---

[5] Had we focused on specific physical models we could use the wavefunction of the universe to obtain corresponding theoretical priors, see [18] for work in this direction.

[6] The momenta and multipoles are related via $q = l/r_h$, where $r_h = 14.2$ Gpc is the comoving radius of the last scattering surface.

$-0.009 < g_{\min} < -0.45$. The prior for β is fixed by using the results from (our fit to) WMAP data. We use two sets of priors: one coming from the 1σ range ($0 \leq \ln\beta \leq 2$) and the other from the 2σ range ($-0.2 \leq \ln\beta \leq 3.5$).

The results for the Bayesian evidence are presented in Fig. 3 for $l \geq 30$, where 2-loop predictions (2) can be trusted. As a guide [69], a difference $\ln E < 1$ is insignificant and $2.5 < \ln E < 5$ is strongly significant. We see that the difference between evidence for ΛCDM and HC predictions is insignificant, with marginal preference for HC, depending on the choice of priors.
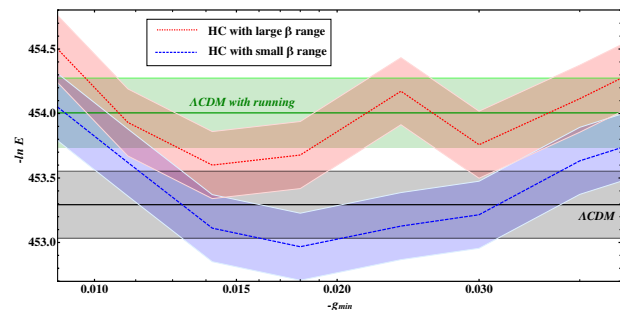

FIG. 3. Bayesian Evidence using $l \geq 30$ data only, where the perturbative expansion (2) can be trusted. Error is indicated by the shaded region around the lines.

Model selection.— We would like now to examine whether we can use the data to rule out or in some of the models described by (3). There are phenomenological and theoretical constraints that we need to satisfy. The phenomenological constraints are: the bound on the tensor-to-scalar ratio, $r \leq 0.125$, should be satisfied, and the model should reproduce the observed values for the amplitude Δ_0^2 and $\ln\beta$. The theoretical prediction for the r is [9, 10, 34],

$$r = 32 \frac{1 + \sum_{M=1}^{\mathcal{N}_\Phi}(1 - 8\xi_M)^2}{1 + 2\mathcal{N}_\psi + \mathcal{N}_\Phi}, \tag{10}$$

and the theoretical predictions for Δ_0^2 and $\ln\beta$ are given in (6-9). In deriving (2) we used a 't Hooft large N expansion and perturbation theory in g_{eff}^2. We thus need to check that any solution of the phenomenological constraints is consistent with these theoretical assumptions.

There are a few universal properties of the 2-loop correction, $gq_*/q \ln|q/\beta gq_*|$. This term vanishes at large q, reflecting the fact that the QFTs we consider are super-renormalizable. Its absolute value gradually increases till it reaches the local maximum $1/e\beta$ at $q = e\beta|g|q_*$. At lower values of l the 2-loop term changes sign and grows very fast as we go to lower multipoles becoming equal to one (same size as the 1-loop contribution) below $l = 10$. Therefore, we should not trust these models below $l \sim 10$. In fact, one should even be cautious in using the 2-loop approximation for l's lower than 35. While the overall

magnitude of the 2-loop term is small up until $l = 10$ this happens due to large cancellation between the f_1 and the f_2 term in (5). We will use as an indicator of the reliability of perturbation theory the size of $f_1 g_{\text{eff}}^2 \ln g_{\text{eff}}^2$.

Let us consider gauge theory coupled to a large number, $\mathcal{N}_\Phi$, of non-mimimal scalars, all with the same non-minimality parameter ξ and the same quartic coupling λ. For sufficiently large $\mathcal{N}_\Phi$, the scalar-to-tensor ratio (10) becomes

$$r = 32(1 - 8\xi)^2 \qquad (11)$$

and the bound on r implies, $|1 - 8\xi| \leq 0.061$, where the equality holds when $r = 0.12$. Choosing a value of ξ, then the observational values of Δ_0^2 and $\ln \beta$ give two equations, which can always be solved to determine N and $\mathcal{N}_\Phi$. For example, if we choose $\xi = 0.133$, which correspond to $r = 0.12$, and take $\lambda = 1$ the solution to the two constraints is

$$N = 2995, \qquad \mathcal{N}_\Phi = 23255. \qquad (12)$$

This solution satisfies the theoretical constraints: firstly, $N^2 \gg \mathcal{N}_\Phi$, so the large N expansion is justified and secondly, the effective coupling remains small for all momenta seen by Planck, $3.3 \times 10^{-4} \leq g_{\text{eff}}^2(q) \leq 0.41$. For this solution however $f_1 \approx -8(1 - 48\xi^2)/(1 - 8\xi)^2 \approx -11$ and $f_1 g_{\text{eff}}^2 \ln g_{\text{eff}}^2 \approx 1$ when $l = 35$, so we should not trust the perturbative expansion below around $l \approx 35$.

Conclusions.— We showed that holographic models based on three-dimensional perturbative QFT are capable of explaining the CMB data and are competitive to ΛCDM model. However, at very low multipoles (roughly $l < 30$), the perturbative expansion breaks down and in this regime the prediction of the theory cannot be trusted. The data are consistent with the dual theory being gauge theory coupled to a large number of nearly conformal scalars with a quartic interaction. It would be interesting to further analyze these models in order to extract other properties that may be testable against observations. In particular, non-perturbative methods (such as putting the dual QFT on a lattice) can be used to reliably model the very low multipoles, which may potentially explain the apparent large angle anomalies in the CMB sky (e.g., [70]).

Appendix: $\langle TT \rangle$ at 2-loops

The holographic formula for the power spectrum reads,

$$\Delta_{\mathcal{R}}^2(q) = -\frac{q^3}{4\pi^2} \frac{1}{\text{Im}\langle\langle T(q)T(-q)\rangle\rangle}, \qquad (13)$$

where $T = T_i^i$ is the trace of the energy momentum tensor and the double bracket notation indicates that the momentum conserving delta function (times $(2\pi)^3$) has been removed. The imaginary part in (13) is taken after analytic continuation

$$q \to -iq, N \to -iN, \qquad (14)$$

where q is the magnitude of the momentum. This formula was derived in [9] using the domain-wall/cosmology correspondence and also follows from the wave-function of the universe approach. There is a similar holographic formula for the tensor power spectrum involving the transverse traceless part of the 2-point function of T_{ij}.

This class of theories we consider has the important property that if one promotes g_{YM}^2 to a new field that transforms appropriately under conformal transformation, the theory becomes conformally invariant [71, 72]. We say that the theory has a "generalized conformal structure". This is not a bona fide symmetry of the theory but, nevertheless, controls many of its properties. The generalised conformal structure implies that the 2-point function of the energy momentum tensor, to leading order in the large N limit (planar diagrams), is given by

$$\langle\langle T(q)T(-q)\rangle\rangle = q^3 N^2 f(g_{\text{eff}}^2), \qquad (15)$$

where $g_{\text{eff}}^2 = g_{YM}^2 N/q$ is the effective dimensionless 't Hooft coupling constant and $f(g_{\text{eff}}^2)$ is function of g_{eff}^2 [72]. The overall factor of q^3 reflects the fact that the energy momentum has dimension 3 in three dimensions and the overall factor of N^2 is because this is the leading order term in the large N limit. Under the analytic continuation (14),

$$g_{\text{eff}}^2(q) \to g_{\text{eff}}^2(q), \quad N^2 q^3 \to -iN^2 q^3 \qquad (16)$$

and therefore for this class of theories,

$$\Delta_{\mathcal{R}}^2(q) = \frac{1}{4\pi^2 N^2 f(g_{eff}^2)}, \qquad (17)$$

which is the formula we used in the main text.

Perturbation theory is valid when $g_{\text{eff}}^2 \ll 1$. In the perturbative regime, the function $f(g_{\text{eff}}^2)$ is given by

$$f(g_{\text{eff}}^2) = f_0 \left(1 - f_1\, g_{\text{eff}}^2 \ln g_{\text{eff}}^2 + f_2\, g_{\text{eff}}^2 + O(g_{\text{eff}}^4)\right). \quad (18)$$

The function f_0 is determined by a 1-loop computation, while f_1 and f_2 come from 2-loops. The presence of the logarithm is due to UV and IR divergences in the computation of the 2-point function of the energy momentum tensor.

The 1-loop computation was done in [9, 10] and we summarize the 2-loop computation of [41] here. Since this a gauge theory we first need to gauge fix. The gauged fixed action is

$$S = \frac{1}{g_{\text{YM}}^2} \int d^3x\, \text{tr} \left[\frac{1}{2} F_{ij} F^{ij} + (\partial^i A_i)^2 + 2\partial^i \bar{c} \mathcal{D}_i c \right.$$
$$+ (\mathcal{D}\Phi^M)^2 + 2\bar{\psi}^L \mathcal{D}\psi^L + 2\sqrt{2}\, \mu_{ML_1 L_2} \Phi^M \bar{\psi}^{L_1} \psi^{L_2}$$
$$\left. + \frac{1}{6} \lambda_{M_1 M_2 M_3 M_4} \Phi^{M_1} \Phi^{M_2} \Phi^{M_3} \Phi^{M_4} \right]. \quad (19)$$

where b, c is the ghost sector. The energy-momentum tensor is obtained by coupling the theory to a background metric g_{ij} and then using $T_{ij} = (2/\sqrt{g})(\delta S/\delta g^{ij})|_{g_{ij}=\delta_{ij}}$. This procedure defines a unique energy momentum tensor, except that there is a choice of how to couple the scalars to gravity. One may include the non-minimal coupling $1/(2g_{\text{YM}}^2) \sum_M \xi_M R(\Phi^M)^2$ in the action, where the sum is over all scalars and different scalars may have a different ξ_M. The variation of this term contributes an "improvement term" to the energy momentum tensor. If $\xi_M = 0$ the scalar is a called a minimal scalar, while if $\xi_M = 1/8$ it is a conformal scalar. The energy momentum obtained in this fashion is given by

$$T_{ij} = T_{ij}^A + T_{ij}^{g.f.} + T_{ij}^{gh} + T_{ij}^{\psi} + T_{ij}^{\Phi} + T_{ij}^Y, \quad (20)$$

where the different terms denote, respectively, the contribution of the gauge fields, the gauge-fixing term , the ghost sector, the fermions, the scalars and the Yukawa

interactions. These are explicitly given by

$$T_{ij}^A = \frac{1}{g_{\text{YM}}^2} \text{tr} \left[F_{ik} F_{jk} - \delta_{ij} \frac{1}{4} F_{kl} F_{kl} \right], \quad (21)$$

$$T_{ij}^{g.f.} = \frac{1}{g_{\text{YM}}^2} \text{tr} \left[A_i \partial_j (\partial_k A_k) + A_j \partial_i (\partial_k A_k) \right.$$
$$\left. - \delta_{ij} \left(A_k\ \partial_k \partial_l A_l + \frac{1}{2} (\partial_k A_k)(\partial_l A_l) \right) \right],$$

$$T_{ij}^{gh} = \frac{1}{g_{\text{YM}}^2} \text{tr} \left[\partial_i \bar{c} \mathcal{D}_j c + \partial_j \bar{c} \mathcal{D}_i c - \delta_{ij} \partial_k \bar{c} \mathcal{D}_k c \right],$$

$$T_{ij}^{\psi} = \frac{1}{g_{\text{YM}}^2} \text{tr} \left[\frac{1}{2} \bar{\psi}^L \gamma_{(i} \overset{\leftrightarrow}{\mathcal{D}}_{j)} \psi^L - \delta_{ij} \frac{1}{2} \bar{\psi}^L \gamma_k \overset{\leftrightarrow}{\mathcal{D}}_k \psi^L \right],$$

$$T_{ij}^{\Phi} = \frac{1}{g_{\text{YM}}^2} \text{tr} \left[\mathcal{D}_i \Phi^M \mathcal{D}_j \Phi^M - \delta_{ij} \left(\frac{1}{2} (\mathcal{D}\Phi^M)^2 \right. \right.$$
$$\left. + \frac{1}{4!} \lambda_{M_1 M_2 M_3 M_4} \Phi^{M_1} \Phi^{M_2} \Phi^{M_3} \Phi^{M_4} \right)$$
$$\left. + \xi_M \left(\delta_{ij} \partial^2 - \partial_i \partial_j \right) (\Phi^M)^2 \right],$$

$$T_{ij}^Y = \frac{1}{g_{\text{YM}}^2} \text{tr} \left[-\delta_{ij}\, \mu_{ML_1 L_2} \Phi^M \bar{\psi}^{L_1} \psi^{L_2} \right].$$

The topology of the 2-loop diagrams that need to be computed is given in Fig. 4. The 2-point function has a
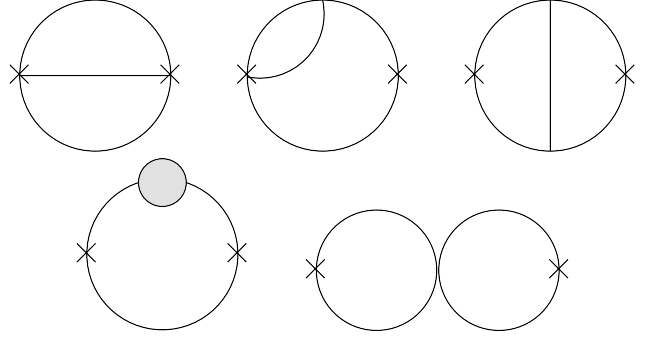

FIG. 4. 2-loop diagrams contributing to $\langle TT \rangle$. The blob in the fourth diagram represents an insertion of a 1-loop self-energy.

UV divergence that can be cancelled by the counterterm

$$a_{CT} \int d^3x \sqrt{g} R, \quad (22)$$

where R is the curvature scalar of the background metric g_{ij}, with appropriately chosen a_{CT}. As usual, this process introduces a renormalization scale μ, which leads to scheme dependence. The correlator also has an IR divergence (unless all scalars are minimal), which we regulated with an IR cut-off, μ_*. This leads to the following result for $\ln \beta$,

$$\ln \beta = \ln \frac{1}{|g|} - \frac{a_0}{f_1} - \left(\ln \frac{q_*}{\mu} + \frac{64/\pi^2}{f_1 \mathcal{N}_{(B)}} \Sigma_\Phi \ln \frac{\mu}{\mu_*} \right), \quad (23)$$

where we have made use of the definition of g, $gq_* = f_1 g_{\text{YM}}^2 N$. The renormalization scale μ is arbitrary and

so is the pivot scale q_*. We fix this scheme dependence by setting, $\mu = q_*$. An alternative scheme is to set μ to the (inverse of the) smallest scale in the data (i.e. equal to 0.17 Mpc^{-1}). We have checked that the results we present in the main text are not sensitive to the choice of scheme, except possibly at very low l's. As argued in the main text, this is precisely the regime where one should not trust the perturbative computation. Regarding the IR divergence now. It was argued in [73, 74] that superrenormalizable theories with a dimensionful coupling constant (as in our case) are non-perturbative IR finite, with $g_{\rm YM}^2$ providing the IR cut-off . We therefore set $\mu_* = c g_{\rm YM}^2$, where c is a number that can only be determined non-perturbatively. This leads to our final formula for $\ln \beta$,

$$\ln \beta = \ln \frac{1}{|g|} - \frac{a_0}{f_1} - \frac{64/\pi^2}{f_1 \mathcal{N}_{(B)}} \Sigma_\Phi \ln \frac{N f_1}{cg} \qquad (24)$$

In the main text we set $c = 1$ but we also checked that the results do not change qualitatively if we change c. An alternative way to deal with the IR issues is to get μ_* equal to the (inverse of the) largest scale in the data (i.e. 1.4×10^{-4} Mpc^{-1}). As in the case of scheme dependence, we have checked that the results are not very sensitive to how we treat μ_*, except possibly at very low ls.

[1] G. 't Hooft, in *Salamfest 1993:0284-296* (1993) pp. 0284–296, arXiv:gr-qc/9310026 [gr-qc].
[2] L. Susskind, J. Math. Phys. **36**, 6377 (1995), arXiv:hep-th/9409089 [hep-th].
[3] J. M. Maldacena, Int. J. Theor. Phys. **38**, 1113 (1999), [Adv. Theor. Math. Phys.2,231(1998)], arXiv:hep-th/9711200 [hep-th].
[4] C. M. Hull, JHEP **07**, 021 (1998), arXiv:hep-th/9806146 [hep-th].
[5] E. Witten, in *Strings 2001: International Conference Mumbai, India, January 5-10, 2001* (2001) arXiv:hep-th/0106109 [hep-th].
[6] A. Strominger, JHEP **10**, 034 (2001), arXiv:hep-th/0106113 [hep-th].
[7] A. Strominger, JHEP **11**, 049 (2001), arXiv:hep-th/0110087 [hep-th].
[8] J. M. Maldacena, JHEP **05**, 013 (2003), arXiv:astro-ph/0210603 [astro-ph].
[9] P. McFadden and K. Skenderis, Phys. Rev. **D81**, 021301 (2010), arXiv:0907.5542 [hep-th].
[10] P. McFadden and K. Skenderis, *Classical and quantum gravity. Proceedings, 1st Mediterranean Conference, MCCQG 2009, Kolymbari, Crete, Greece, September 14-18, 2009*, J. Phys. Conf. Ser. **222**, 012007 (2010), arXiv:1001.2007 [hep-th].
[11] P. McFadden and K. Skenderis, JCAP **1105**, 013 (2011), arXiv:1011.0452 [hep-th].
[12] P. McFadden and K. Skenderis, JCAP **1106**, 030 (2011), arXiv:1104.3894 [hep-th].
[13] A. Bzowski, P. McFadden, and K. Skenderis, JHEP **03**, 091 (2012), arXiv:1112.1967 [hep-th].
[14] K. Skenderis and P. K. Townsend, Phys. Rev. Lett. **96**, 191301 (2006), arXiv:hep-th/0602260 [hep-th].
[15] J. Garriga, K. Skenderis, and Y. Urakawa, JCAP **1501**, 028 (2015), arXiv:1410.3290 [hep-th].
[16] J. M. Maldacena and G. L. Pimentel, JHEP **09**, 045 (2011), arXiv:1104.2846 [hep-th].
[17] J. B. Hartle, S. W. Hawking, and T. Hertog, (2012), arXiv:1205.3807 [hep-th].
[18] J. B. Hartle, S. W. Hawking, and T. Hertog, JCAP **1401**, 015 (2014), arXiv:1207.6653 [hep-th].
[19] K. Schalm, G. Shiu, and T. van der Aalst, JCAP **1303**, 005 (2013), arXiv:1211.2157 [hep-th].
[20] A. Bzowski, P. McFadden, and K. Skenderis, JHEP **04**, 047 (2013), arXiv:1211.4550 [hep-th].
[21] I. Mata, S. Raju, and S. Trivedi, JHEP **07**, 015 (2013), arXiv:1211.5482 [hep-th].
[22] J. Garriga and Y. Urakawa, JCAP **1307**, 033 (2013), arXiv:1303.5997 [hep-th].
[23] P. McFadden, JHEP **10**, 071 (2013), arXiv:1308.0331 [hep-th].
[24] A. Ghosh, N. Kundu, S. Raju, and S. P. Trivedi, JHEP **07**, 011 (2014), arXiv:1401.1426 [hep-th].
[25] J. Garriga and Y. Urakawa, JHEP **06**, 086 (2014), arXiv:1403.5497 [hep-th].
[26] N. Kundu, A. Shukla, and S. P. Trivedi, JHEP **04**, 061 (2015), arXiv:1410.2606 [hep-th].
[27] P. McFadden, JHEP **02**, 053 (2015), arXiv:1412.1874 [hep-th].
[28] N. Arkani-Hamed and J. Maldacena, (2015), arXiv:1503.08043 [hep-th].
[29] N. Kundu, A. Shukla, and S. P. Trivedi, JHEP **01**, 046 (2016), arXiv:1507.06017 [hep-th].
[30] T. Hertog and E. van der Woerd, JCAP **1602**, 010 (2016), arXiv:1509.03291 [hep-th].
[31] J. Garriga, Y. Urakawa, and F. Vernizzi, JCAP **1602**, 036 (2016), arXiv:1509.07339 [hep-th].
[32] J. Garriga and Y. Urakawa, (2016), arXiv:1606.04767 [hep-th].
[33] C. Corianò, L. Delle Rose, and M. Serino, JHEP **12**, 090 (2012), arXiv:1210.0136 [hep-th].
[34] S. Kawai and Y. Nakayama, JHEP **06**, 052 (2014), arXiv:1403.6220 [hep-th].
[35] R. Easther, R. Flauger, P. McFadden, and K. Skenderis, JCAP **1109**, 030 (2011), arXiv:1104.2040 [astro-ph.CO].
[36] A. Kosowsky and M. S. Turner, Phys. Rev. **D52**, 1739 (1995), arXiv:astro-ph/9504071 [astro-ph].
[37] E. Komatsu *et al.* (WMAP), Astrophys. J. Suppl. **192**, 18 (2011), arXiv:1001.4538 [astro-ph.CO].
[38] M. Dias, Phys. Rev. **D84**, 023512 (2011), arXiv:1104.0625 [astro-ph.CO].
[39] P. A. R. Ade *et al.* (Planck), (2015), arXiv:1502.01589 [astro-ph.CO].
[40] N. Afshordi, E. Gould, and K. Skenderis, (2016), to appear.
[41] C. Corianò, L. Delle Rose, and K. Skenderis, (2016), to appear.
[42] See Supplemental Material at [URL will be inserted by publisher] for technical details.
[43] U. Seljak and M. Zaldarriaga, Astrophys. J. **469**, 437 (1996), astro-ph/9603033.
[44] M. Zaldarriaga, U. Seljak, and E. Bertschinger, Astrophys.J. **494**, 491 (1998), arXiv:astro-ph/9704265 [astro-ph].
[45] A. Lewis, A. Challinor, and A. Lasenby, Astrophys. J.

538, 473 (2000), arXiv:astro-ph/9911177 [astro-ph].

[46] A. Lewis and S. Bridle, Phys. Rev. **D66**, 103511 (2002), arXiv:astro-ph/0205436 [astro-ph].

[47] C. Howlett, A. Lewis, A. Hall, and A. Challinor, JCAP **1204**, 027 (2012), arXiv:1201.3654 [astro-ph.CO].

[48] A. Lewis, Phys. Rev. **D87**, 103529 (2013), arXiv:1304.4473 [astro-ph.CO].

[49] A. Lewis, "CAMB Notes," `http://cosmologist.info/notes/CAMB.pdf`.

[50] P. Ade *et al.* (Planck), (2015), arXiv:1502.01591 [astro-ph.CO].

[51] N. Aghanim *et al.* (Planck), (2015), arXiv:1507.02704 [astro-ph.CO].

[52] P. Ade *et al.* (Planck), (2015), arXiv:1502.01597 [astro-ph.CO].

[53] C. Bennett *et al.* (WMAP), Astrophys.J.Suppl. **208**, 20 (2013), arXiv:1212.5225 [astro-ph.CO].

[54] C. Reichardt, L. Shaw, O. Zahn, K. Aird, B. Benson, *et al.*, Astrophys.J. **755**, 70 (2012), arXiv:1111.0932 [astro-ph.CO].

[55] S. Das, T. Louis, M. R. Nolta, G. E. Addison, E. S. Battistelli, *et al.*, JCAP **1404**, 014 (2014), arXiv:1301.1037 [astro-ph.CO].

[56] F. Beutler, C. Blake, M. Colless, D. H. Jones, L. Staveley-Smith, *et al.*, Mon.Not.Roy.Astron.Soc. **416**, 3017 (2011), arXiv:1106.3366 [astro-ph.CO].

[57] C. Blake, E. Kazin, F. Beutler, T. Davis, D. Parkinson, *et al.*, Mon.Not.Roy.Astron.Soc. **418**, 1707 (2011), arXiv:1108.2635 [astro-ph.CO].

[58] L. Anderson *et al.*, Mon. Not. Roy. Astron. Soc. **427**, 3435 (2013), arXiv:1203.6594 [astro-ph.CO].

[59] F. Beutler, C. Blake, M. Colless, D. H. Jones, L. Staveley-Smith, *et al.*, Mon.Not.Roy.Astron.Soc. **423**, 3430 (2012), arXiv:1204.4725 [astro-ph.CO].

[60] N. Padmanabhan, X. Xu, D. J. Eisenstein, R. Scalzo, A. J. Cuesta, K. T. Mehta, and E. Kazin, Mon. Not. Roy. Astron. Soc. **427**, 2132 (2012), arXiv:1202.0090 [astro-ph.CO].

[61] L. Anderson *et al.* (BOSS), Mon. Not. Roy. Astron. Soc. **441**, 24 (2014), arXiv:1312.4877 [astro-ph.CO].

[62] L. Samushia, B. A. Reid, M. White, W. J. Percival, A. J. Cuesta, *et al.*, Mon.Not.Roy.Astron.Soc. **439**, 3504 (2014), arXiv:1312.4899 [astro-ph.CO].

[63] A. J. Ross, L. Samushia, C. Howlett, W. J. Percival, A. Burden, and M. Manera, Mon. Not. Roy. Astron. Soc. **449**, 835 (2015), arXiv:1409.3242 [astro-ph.CO].

[64] P. Ade *et al.* (BICEP2, Planck), Phys.Rev.Lett. **114**, 101301 (2015), arXiv:1502.00612 [astro-ph.CO].

[65] M. Powell, "The BOBYQA algorithm for bound constrained optimization without derivatives," `http://www.damtp.cam.ac.uk/user/na/NA_papers/NA2009_06.pdf`.

[66] F. Feroz and M. P. Hobson, Mon. Not. Roy. Astron. Soc. **384**, 449 (2008), arXiv:0704.3704 [astro-ph].

[67] F. Feroz, M. P. Hobson, and M. Bridges, Mon. Not. Roy. Astron. Soc. **398**, 1601 (2009), arXiv:0809.3437 [astro-ph].

[68] F. Feroz, M. P. Hobson, E. Cameron, and A. N. Pettitt, (2013), arXiv:1306.2144 [astro-ph.IM].

[69] R. Trotta, Contemp. Phys. **49**, 71 (2008), arXiv:0803.4089 [astro-ph].

[70] P. A. R. Ade *et al.* (Planck), Astron. Astrophys. **571**, A23 (2014), arXiv:1303.5083 [astro-ph.CO].

[71] A. Jevicki, Y. Kazama, and T. Yoneya, Phys. Rev. **D59**, 066001 (1999), arXiv:hep-th/9810146 [hep-th].

[72] I. Kanitscheider, K. Skenderis, and M. Taylor, JHEP **09**, 094 (2008), arXiv:0807.3324 [hep-th].

[73] R. Jackiw and S. Templeton, Phys. Rev. **D23**, 2291 (1981).

[74] T. Appelquist and R. D. Pisarski, Phys. Rev. **D23**, 2305 (1981).